Hindawi Publishing Corporation
International Journal of Rotating Machinery
Volume 2007, Article ID 27247, 11 pages
doi:10.1155/2007/27247

Research Article

A Class of Methods for the Analysis of Blade Tip Timing Data from Bladed Assemblies Undergoing Simultaneous Resonances—Part I: Theoretical Development

J. Gallego-Garrido,[1] G. Dimitriadis,[2] and J. R. Wright[2]

[1] *Experimental Vibrations, Rolls-Royce PLC, P.O. Box 31, Derby DE24 8DJ, UK*
[2] *School of Mechanical Aerospace and Civil Engineering, University of Manchester, Simon Building, Oxford Road, Manchester M13 9PL, UK*

Received 6 March 2006; Revised 17 November 2006; Accepted 4 January 2007

Recommended by Eric Maslen

Blade tip timing is a technique for the measurement of vibrations in rotating bladed assemblies. Although the fundamentals of the technique are simple, the analysis of data obtained in the presence of simultaneously occurring synchronous resonances is problematic. A class of autoregressive-based methods for the analysis of blade tip timing data from assemblies undergoing two simultaneous resonances has been developed. It includes approaches that assume both sinusoidal and general blade tip responses. The methods can handle both synchronous and asynchronous resonances. An exhaustive evaluation of the approaches was performed on simulated data in order to determine their accuracy and sensitivity. One of the techniques was found to perform best on asynchronous resonances and one on synchronous resonances. Both methods yielded very accurate vibration frequency estimates under all conditions of interest.

1. INTRODUCTION

Blade tip timing (BTT) is a vibration measurement technology that can be used to identify vibration problems in bladed assemblies through measurement of the passing times of blade tips under stationary points. The aim of researching and developing BTT vibration measurement systems is to provide technically feasible cost-effective means to identify causes of potential blade failures. Blade tip timing has the potential to overcome many of the limitations of currently well-established systems, providing more information at a fraction of the cost.

However, the recovery of the vibration information is complex because the analysis techniques differ depending on the type of blade response being sampled. The main recent focus of BTT data analysis research has been the determination of frequencies when the vibration of the blades is synchronous. Synchronous vibration, also known as integral-ordered or engine-ordered (EO) resonance, occurs when the response frequency of the blades is an integer multiple of the rotational speed of the assembly. During synchronous resonance, the probes always detect the blade at the same phase of the vibration cycle, thus limiting the amount of data that is available for the estimation of the response frequency and amplitude.

A number of methods have been proposed for the analysis of BTT data from assemblies undergoing synchronous vibrations, such as the single parameter technique developed by Zablotskiy and Korostelev [1], the two-parameter plot method (Heath et al. [2]), the technique by Zielinski and Ziller [3], and various autoregressive methods (Dimitriadis et al. [4], Carrington et al. [5], the authors [6], Gallego-Garrido and Dimitriadis [7]).

The problem of synchronous resonance is further complicated when two or more modes of vibration resonate simultaneously. This is not an uncommon event and has been repeatedly reported in the literature regarding aeroengine vibration problems since the early investigations of Armstrong and Stevenson [8]. Autoregressive-based methods and the two-parameter plot method have been shown to fail when two simultaneous synchronous resonances from simulated BTT data are analysed (the authors [6]).

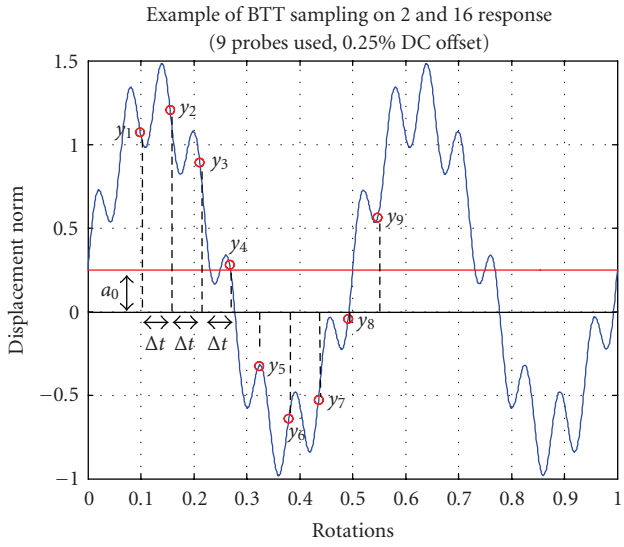

Figure 1: Relationship of sampling points to data points.

Virtually no detailed information on the recovery of multiple frequencies from BTT data exists in the public domain. A few techniques were developed at Rolls-Royce PLC over the last 30 years but never published externally. Robinson [9, 10] reported the existence at Pratt and Whitney of techniques for decoupling two simultaneously occurring synchronous modes. In literature, reporting the current capabilities of BTT systems used by partners in the High Cycle Fatigue programme and the Propulsion Instrumentation Working Group, the issue of simultaneous multimode capability is often referred to (Jones [11], Hayes et al. [12]). However, there is no clear statement that this capability is fully implemented and has been used successfully. In a white paper, Jones [11] described that the expected capabilities of a 4th generation NSMS[1] system (Gen IV) would include an offline simultaneous mode capability. Hayes et al. [12] reported that the current capabilities of the 4th generation system include the ability to recover up to 5 simultaneous modes in offline analysis depending on the number of probes used; however, no description of the methodology is given.

This paper presents a new class of methods for the analysis of BTT data from assemblies undergoing two simultaneous resonances. The techniques are based on an autoregressive framework. The methods are demonstrated and validated on simulated data.

2. BASIC METHODOLOGY (MAR)

The autoregressive (AR) model can be applied to a set of sampled output data in order to identify a given output-only dynamic system. The multiple-frequency autoregressive (MAR) BTT method is based on the linear-prediction autoregressive equation for a multi-degree-of-freedom system with J modes

$$y_i = a_0 - \sum_{m=1}^{2J} a_m y_{(i-m)}, \tag{1}$$

where y_i are the observations made, a_m are the autoregressive coefficients, and a_0 is the constant offset. The notation $y_{(i-m)}$ denotes observations recorded earlier than y_i by m time steps, that is, $m\Delta t$, where Δt is the time step. Equation (1) is only valid in the case where Δt is a constant. Since the measurements y are obtained by means of BTT probes, the constant time step requirement can be translated to a constant spacing of the probes around the circumference of the bladed assembly, provided the rotational speed of the assembly is approximately constant or varying very slowly.

Equation (1) can be put in matrix form for N observations of y, thus giving

$$\begin{bmatrix} y_{2J+1} \\ y_{2J+2} \\ \vdots \\ y_N \end{bmatrix} = \begin{bmatrix} -y_{2J} & -y_{2J-1} & \cdots & -y_1 & 1 \\ -y_{2J+1} & -y_{2J} & \cdots & -y_2 & 1 \\ \vdots & \vdots & \ddots & \vdots & \vdots \\ -y_{N-1} & -y_{N-2} & \cdots & -y_{N-2J} & 1 \end{bmatrix} \begin{bmatrix} a_1 \\ a_2 \\ \vdots \\ a_{2J} \\ a_0 \end{bmatrix} \tag{2}$$

or in short notation

$$\mathbf{y} = \mathbf{Ha}. \tag{3}$$

The autoregressive model of (1) is fully defined when the a_m coefficients are evaluated by solving (3). There are $2J + 1$ unknowns requiring at least $2J + 1$ equations. In terms of BTT probes, this means that a minimum of $N_{\min}$ probes is required, where $N_{\min}$ is given by

$$N_{\min} = 4J + 1. \tag{4}$$

For example, if two frequencies are to be extracted from the data, the minimum number of observations, that is, probes, will be 9 and (2) is written as

$$\begin{bmatrix} y_5 \\ y_6 \\ y_7 \\ y_8 \\ y_9 \end{bmatrix} = \begin{bmatrix} -y_4 & -y_3 & -y_2 & -y_1 & 1 \\ -y_5 & -y_4 & -y_3 & -y_2 & 1 \\ -y_6 & -y_5 & -y_4 & -y_3 & 1 \\ -y_7 & -y_6 & -y_5 & -y_4 & 1 \\ -y_8 & -y_7 & -y_6 & -y_5 & 1 \end{bmatrix} \begin{bmatrix} a_1 \\ a_2 \\ a_3 \\ a_4 \\ a_0 \end{bmatrix}. \tag{5}$$

The data points in (5) are plotted graphically in Figure 1, as they would be measured by a BTT system. The figure shows a continuous signal made up of two sine waves with different frequencies, amplitudes, and phases, sampled by nine BTT probes. The constant term a_0 corresponds to a constant blade offset which occurs due to aerodynamic loading and other factors. Estimating or removing the blade offset prior to the analysis of the data will translate into a reduction to the number of required probes.

[1] Noncontacting stress measurement system (NSMS) is the United States Air Force term for BTT.

The system of (5) can be solved directly or in a least squares sense in the case where there are more than the minimum number of probes or where data from more than one revolution is used. Using the notation in (3)

$$\mathbf{a} = (\mathbf{H}^{\mathrm{T}}\mathbf{H})^{-1}\mathbf{H}^{\mathrm{T}}\mathbf{y}. \tag{6}$$

2.1. Frequency estimation by Prony's method

The frequency estimates from the MAR formulation for BTT data analysis are obtained by means of Prony's method. The method assumes that a sample of data can be represented as a sum of damped exponentials. The method has been adapted to suit the BTT problem by assuming that the exponentials are undamped when the blade is undergoing forced resonance, so that the real parts of the exponential solution can be discarded.

It can be shown that the elements $a_1, a_2, a_3, \ldots, a_{2J}$ in the solution vector of coefficients $\mathbf{a}$ are the coefficients of the characteristic equation that defines the decay response motion of a J-degree of freedom dynamic system (Marple [13])

$$\mu^{2J} + a_1\mu^{2J-1} + a_2\mu^{2J-2} + \cdots + a_{2J} = 0. \tag{7}$$

The solution for the roots is

$$\mu_j = e^{-\varsigma_j\omega_j\Delta t + i\omega_{dj}\Delta t} = e^{\lambda_j\Delta t}, \tag{8}$$

where μ_j is the jth solution of the characteristic equation, λ_j is the jth eigenvalue of the vibrating system, ω_j is the jth frequency of vibration, ζ_j is the jth damping ratio, and $\omega_{dj} = \omega_j\sqrt{1-\varsigma_j^2}$ is the jth damped frequency of vibration. The characteristic equation has $2J$ solutions, leading to J complex conjugate pairs $\lambda_1, \lambda_1^*, \lambda_2, \lambda_2^*, \lambda_3, \lambda_3^*, \ldots, \lambda_J, \lambda_J^*$ for the system eigenvalues.

In the presence of high levels of noise, the term $(\mathbf{H}^{\mathrm{T}}\mathbf{H})$ in (6) can become badly conditioned, thus causing inaccuracies in the estimation of the a_m coefficients, which in turn will affect the estimation of μ_j from (7). In that case, it can happen that the resulting eigenvalues λ_j are not complex conjugate pairs. Hence only the recovered eigenvalues that come in complex conjugate pairs are accepted during the BTT data analysis procedure. Eigenvalues which do not conform to this condition are discarded. Another approach to determining the quality of the estimates exists, by which the eigenvalues are plotted on the complex plane. The acceptable estimates will lie outside the unit circle, while the estimates produced by noise will lie inside the unit circle (Marple [13]).

For the application of the technique to BTT data, it was decided to assume that the response on the resonance is sinusoidal with constant amplitude. Therefore, it can be simplified by setting $\varsigma_j = 0$ and $\omega_{dj} = \omega_j$ so that

$$\lambda_j = i\omega_j. \tag{9}$$

This simplifies the solution of (8) to

$$\lambda_j = \frac{\ln(\mu_j)}{\Delta t} \tag{10}$$

since the real part has been eliminated from the complex eigenvalues. The jth frequency of vibration is obtained as

$$\omega_j = |\lambda_j|. \tag{11}$$

2.2. Frequency estimation by exact solution

Another way in which the frequency estimates can be improved is by reducing the order of the system in (5). An exact solution can be derived for the special case of sinusoidal motion with two harmonic components. Consider the displacement of the blade tip as the linear superposition of two undamped sinusoids without any offsets:

$$y_i = A_1 \cdot \sin(\omega_1 t_i + \phi_1) + A_2 \cdot \sin(\omega_2 t_i + \phi_2), \tag{12}$$

where y_i is the measured displacement, t_i is the time at which the displacement was calculated, ω_1, ω_2 are the frequencies of vibration of the first and second modes, respectively, A_1, A_2 are the amplitudes and ϕ_1, ϕ_2 are the phases of vibration.

According to this formulation, the $(i-m)$ term in the expansion of the linear prediction shown in (1) would be

$$\begin{aligned} y_{i-m} = {} & A_1 \sin(\omega_1(t_i - m\Delta t) + \phi_1) \\ & + A_2 \sin(\omega_2(t_i - m\Delta t) + \phi_2). \end{aligned} \tag{13}$$

Substitution of the terms in (13) into (1) yields an expression from which the sine and cosine terms can be isolated if a homogenous solution is assumed:

$$\begin{aligned} A_1 \cdot \sin(\omega_1 t + \phi_1) \times (1 + a_1\cos(\omega_1\Delta t) + a_2\cos(\omega_1 2\Delta t) \\ + a_3\cos(\omega_1 3\Delta t) + a_4\cos(\omega_1 4\Delta t)) = 0, \\ A_1 \cdot \cos(\omega_1 t) \times (a_1\sin(\omega_1\Delta t) + a_2\sin(\omega_1 2\Delta t) \\ + a_3\sin(\omega_1 3\Delta t) + a_4\sin(\omega_1 4\Delta t)) = 0, \\ A_2 \cdot \sin(\omega_2 t + \phi_2) \times (1 + a_1\cos(\omega_2\Delta t) + a_2\cos(\omega_2 2\Delta t) \\ + a_3\cos(\omega_2 3\Delta t) + a_4\cos(\omega_2 4\Delta t)) = 0, \\ A_2 \cdot \cos(\omega_2 t + \phi_1) \times (a_1\sin(\omega_2\Delta t) + a_2\sin(\omega_2 2\Delta t) \\ + a_3\sin(\omega_2 3\Delta t) + a_4\sin(\omega_2 4\Delta t)) = 0. \end{aligned} \tag{14}$$

The system of equations in (14) can be solved to find expressions for the autoregressive coefficients a_1, a_2, a_3, a_4:

$$\begin{aligned} a_1 &= -2(\cos(\omega_1\Delta t) + \cos(\omega_2\Delta t)), \\ a_2 &= 2(1 + 2\cos(\omega_1\Delta t)\cos(\omega_2\Delta t)), \\ a_3 &= -2(\cos(\omega_1\Delta t) + \cos(\omega_2\Delta t)), \\ a_4 &= 1. \end{aligned} \tag{15}$$

It is evident that $a_3 = a_1$ and a_4 is known. The result is logical; since there are two unknown frequencies, there will only be two solutions to the system of equations.

Therefore it is only necessary to determine the values of the a_1 and a_2 autoregressive coefficients from the least squares computation. It is also possible to simplify the linear prediction expansion in (1) as

$$y_i + y_{i-4} = -a_1(y_{i-1} + y_{i-3}) - a_2 y_{i-2} + a_0. \tag{16}$$

The system of equations for the exact solution model becomes

$$\begin{bmatrix} y_5 + y_1 \\ y_6 + y_2 \\ y_7 + y_{31} \end{bmatrix} = \begin{bmatrix} -(y_4 + y_2) & -y_3 & 1 \\ -(y_5 + y_3) & -y_4 & 1 \\ -(y_6 + y_4) & -y_5 & 1 \end{bmatrix} \begin{bmatrix} a_1 \\ a_2 \\ a_0 \end{bmatrix}. \quad (17)$$

Notice that the reduction in the order of the system of equations means that less data points are needed with respect to the linear prediction model used for Prony's method. For this exact solution, the minimum number of data points required is:

$$N_{\min} = 4J - 1 \quad (18)$$

corresponding to a reduction of two data points, that is, probes, with respect to the Prony method. In addition, if the blade offsets are known or removed, (18) is reduced to

$$\begin{bmatrix} y_5 + y_1 \\ y_6 + y_2 \end{bmatrix} = \begin{bmatrix} -(y_4 + y_2) & -y_3 \\ -(y_5 + y_3) & -y_4 \end{bmatrix} \begin{bmatrix} a_1 \\ a_2 \end{bmatrix} \quad (19)$$

signifying that only 6 probes are required.

Once a_1 and a_2 have been determined, the frequencies of vibration, ω_1 and ω_2, can be recovered in one of two ways.

(a) Determining the values of a_1, a_2, from (17), deducing a_3 and a_4 from (15), and then using Prony's method, (10), and (11).

(b) Determining the values of a_1, a_2, from (17), and then directly substituting them into (15) to obtain

$$\omega_1 = \arctan\left(\frac{1}{4}\frac{\sqrt{4 - a_1^2 - a_1\sqrt{a_1^2 + 8 + 4a_2} - 2a_2}}{a_1 + \sqrt{a_1^2 + 8 + 4a_2}}\right)\frac{1}{\Delta t},$$

$$\omega_2 = \arctan\left(\frac{1}{4}\frac{\sqrt{4 - a_1^2 - a_1\sqrt{a_1^2 + 8 + 4a_2} - 2a_2}}{a_1 - \sqrt{a_1^2 + 8 + 4a_2}}\right)\frac{1}{\Delta t}. \quad (20)$$

It should be stressed that both (10) and (20) contain Δt, the time step. As with the basic autoregressive method, the time step must be approximately constant.

3. MULTIPLE REVOLUTION FORMULATION (MGAR)

As described up to now, the MAR method uses data from a single revolution of the assembly (this will be referred to as a rev-by-rev approach). Here, the technique will be extended to use data from multiple revolutions and the resulting methodology will be denoted by the initials MGAR. The MGAR formulation improves the MAR frequency estimates by creating an over-determined system of equations. The effect of the over-determination is to reduce the scatter in the least squares estimates, although bias may still be present.

The MGAR formulation assumes that each blade will vibrate at a constant frequency over the range of revolutions used. For such an assumption to be valid, it is also necessary to assume continuity in sampling between different blades and rotations. The number of revolutions to be used depends on the type of test that is being performed on the assembly. If the assembly is run at constant speed, then all the data from all the revolutions can be used in the frequency estimation procedure. If the assembly is being accelerated or decelerated, then the number of revolutions to be used depends on the speed of the manoeuvre and the damping rates of the structure.

Using the same notation as in (3), the multirevolution system of equations is written as

$$\begin{bmatrix} {}^{\text{rev}1}\mathbf{y} \\ \vdots \\ {}^{\text{rev}R}\mathbf{y} \end{bmatrix} = \begin{bmatrix} {}^{\text{rev}1}\mathbf{H} \\ \vdots \\ {}^{\text{rev}R}\mathbf{H} \end{bmatrix} \mathbf{a}, \quad (21)$$

where R is the total number of revolutions used, $\mathbf{y}$ and $\mathbf{H}$ are the data points vectors and matrices; and $\mathbf{a}$ is the vector of unknown autoregressive coefficients. Any of the following schemes can be used in the multirev formulation, namely

(i) Prony with no constant offset,
(ii) Prony with constant offset,
(iii) exact solution with no constant offset,
(iv) exact solution with constant offset.

As an example, the global expansion over two revolutions worth of data for the Prony formulation with offsets when seeking to recover two simultaneous frequencies is given by

$$\begin{bmatrix} {}^1y_5 \\ {}^1y_6 \\ {}^1y_7 \\ {}^1y_8 \\ {}^1y_9 \\ {}^2y_5 \\ {}^2y_6 \\ {}^2y_7 \\ {}^2y_8 \\ {}^2y_9 \end{bmatrix} = \begin{bmatrix} -{}^1y_4 & -{}^1y_3 & -{}^1y_2 & -{}^1y_1 & 1 \\ -{}^1y_5 & -{}^1y_4 & -{}^1y_3 & -{}^1y_2 & 1 \\ -{}^1y_6 & -{}^1y_5 & -{}^1y_4 & -{}^1y_3 & 1 \\ -{}^1y_7 & -{}^1y_6 & -{}^1y_5 & -{}^1y_4 & 1 \\ -{}^1y_8 & -{}^1y_7 & -{}^1y_6 & -{}^1y_5 & 1 \\ -{}^2y_4 & -{}^2y_3 & -{}^2y_2 & -{}^2y_1 & 1 \\ -{}^2y_5 & -{}^2y_4 & -{}^2y_3 & -{}^2y_2 & 1 \\ -{}^2y_6 & -{}^2y_5 & -{}^2y_4 & -{}^2y_3 & 1 \\ -{}^2y_7 & -{}^2y_6 & -{}^2y_5 & -{}^2y_4 & 1 \\ -{}^2y_8 & -{}^2y_7 & -{}^2y_6 & -{}^2y_5 & 1 \end{bmatrix} \begin{bmatrix} a_1 \\ a_2 \\ a_3 \\ a_4 \\ a_0 \end{bmatrix}, \quad (22)$$

where the left superscript denotes the first or second revolutions.

4. MULTIREV AUTOREGRESSIVE WITH INSTRUMENTAL VARIABLES (MGARIV)

As mentioned in the previous section, the inclusion of additional data in the least squares curve-fit decreases the scatter in the results but not necessarily the bias. A simple instrumental variables scheme can be used in order to attempt to decrease the bias.

In this work, an instrumental variables matrix of delayed observations is used. If the delayed observations are defined as

$$z_i = x_{i+\lambda} \quad \text{for } i = 1, 2, 3, \ldots, N, \tag{23}$$

then z_i is the instrumental variable of the measured data x_i. The lag parameter λ represents the delay in the time domain and can be chosen as

$$\lambda = N_{\text{IV}} \times R_{\text{IV}}, \tag{24}$$

where R_{IV} is the number of revolutions, and N_{IV} is the number of equations given by

$$N_{\text{IV}} = N_{\min} - 2J. \tag{25}$$

Equation (21) is rewritten for the instrumental variables formulation as

$$\begin{bmatrix} {}^{\text{rev } 1}\mathbf{y} \\ \vdots \\ {}^{\text{rev } R-\lambda}\mathbf{y} \end{bmatrix} = \begin{bmatrix} {}^{\text{rev } 1}\mathbf{H} \\ \vdots \\ {}^{\text{rev } R-\lambda}\mathbf{H} \end{bmatrix} \mathbf{a} \tag{26}$$

or using the IV subindex to differentiate from previous expressions, it can be written in matrix notation as

$$\mathbf{y}_{\text{IV}} = \mathbf{H}_{\text{IV}} \times \mathbf{a}. \tag{27}$$

The corresponding instrumental variables matrix is constructed by grouping the observation matrices but delayed by λ with respect to those in (24)

$$\mathbf{Z}_\lambda = \begin{bmatrix} {}^{\text{rev } 1+\lambda}\mathbf{H} \\ \vdots \\ {}^{\text{rev } R}\mathbf{H} \end{bmatrix}. \tag{28}$$

Finally, using the usual notation

$$\mathbf{a} = \left(\mathbf{Z}_\lambda^{\text{T}}\mathbf{H}_{\text{IV}}\right)^{-1}\mathbf{Z}_\lambda^{\text{T}}\mathbf{y}_{\text{IV}}. \tag{29}$$

The estimation of the autoregressive coefficients can be made either by Prony's method or the exact solution method.

5. MULTIREV AUTOREGRESSIVE MOVING AVERAGE METHOD (MGARMA)

The autoregressive moving average formulation is also aimed at increasing the robustness of the methods to noise. The ARMA approach acknowledges that a white noise component is present in the linear prediction model.

The general form of an ARMA for a multi-degree-of-freedom system with J modes is

$$\sum_{n=0}^{2J-1} b_n u_{i-n} = y_i + \sum_{m=1}^{2J} a_m y_{i-m}, \tag{30}$$

where y_i are the output observations, u_i is a white noise input, and a_m and b_n are constant coefficients. Equation (30) can be expanded for N observations to give

$$\begin{bmatrix} y_{2J+1} \\ y_{2J+2} \\ \vdots \\ y_N \end{bmatrix} = \begin{bmatrix} -y_{2J} & -y_{2J-1} & \cdots & -y_1 \\ -y_{2J+1} & -y_{2J} & \cdots & -y_2 \\ \vdots & \vdots & \ddots & \vdots \\ -y_{N-1} & -y_{N-2} & \cdots & -y_{N-2J} \end{bmatrix} \times \begin{bmatrix} u_{2J+1} & u_{2J} & \cdots & u_2 \\ u_{2J+2} & u_{2J+1} & \cdots & u_3 \\ \vdots & \vdots & \ddots & \vdots \\ u_N & u_{N-1} & \cdots & u_{N-2J+1} \end{bmatrix} \begin{bmatrix} a_1 \\ a_2 \\ \vdots \\ a_{2J} \\ b_o \\ b_1 \\ \vdots \\ b_{2J-1} \end{bmatrix} \tag{31}$$

or

$$\mathbf{y} = \mathbf{B}\mathbf{c}. \tag{32}$$

The white noise observations $u_1, u_2, \ldots, u_n$ are random entries with a normal distribution of zero mean and unit variance. The system of equations can be solved in a least squares sense to obtain the ARMA coefficients in vector $\mathbf{c}$. However, it can be seen from (31) that the number of equations needed in order to solve the equations is

$$N = (2 \times 2J) + 2J, \tag{33}$$

which indicates that the number of probes required to identify a double resonance would be 12. This is an unrealistically high number for the application of the method to a BTT application. Rather than increasing the number of probes, it was decided to construct the matrix using data from multiple revolutions. Hence the MGARMA is obtained simply by substituting the system in (31) into (21), that is,

$$\begin{bmatrix} {}^{\text{rev } 1}\mathbf{y} \\ \vdots \\ {}^{\text{rev } R}\mathbf{y} \end{bmatrix} = \begin{bmatrix} {}^{\text{rev } 1}\mathbf{B} \\ \vdots \\ {}^{\text{rev } R}\mathbf{B} \end{bmatrix} \mathbf{c}. \tag{34}$$

Notice that the minimum value that R can take is 2. According to Marple [13], it is enough to consider the $a_1, a_2, \ldots, a_{2J}$ coefficients for the estimation of the vibration frequencies. These can be obtained using either the Prony or the exact solution approach.

6. METHOD CLASSIFICATION

Either of the approaches of Sections 2.1 and 2.2 can be used to extract the frequencies from the autoregressive formulations of Sections 2, 3, 4, and 5. Therefore, two classes of methods can be created.

(1) *Prony-based methods*

These are MAR, MGAR, MGARIV, and MGARMA, where all of the a_0, a_1, a_2, a_3, and a_4 coefficients are assumed to be unknown and included in the curve-fit. The frequencies are then estimated using Prony's method, (11).

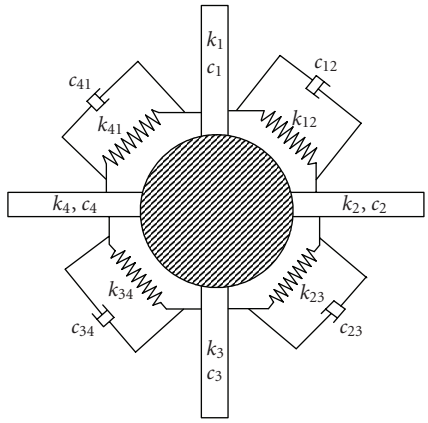

Figure 2: Assembly with four blades.

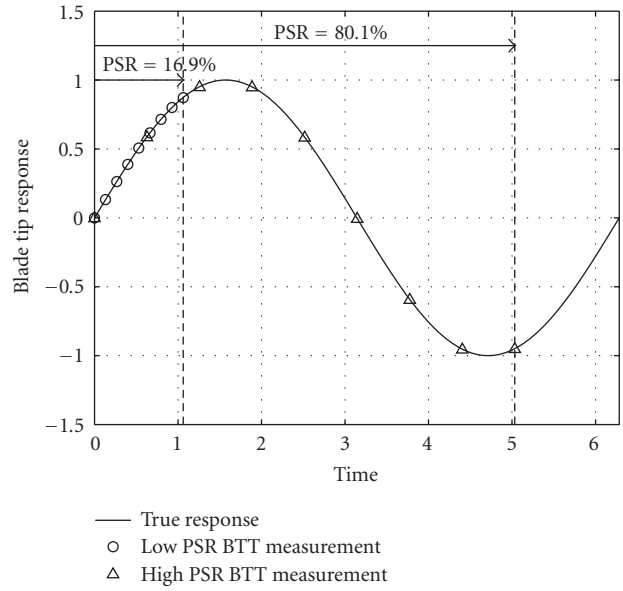

Figure 3: Example of BTT measurements with low and high PSR values.

(2) *Exact methods*

These are MARE, MGARE, and MGARIVE, where only a_0, a_1, and a_2 are assumed to be unknown and included in the curve-fit. The remaining coefficients are obtained from $a_3 = a_1$ and $a_4 = -1$ (see (15)). There are two variants of these exact methods.

(a) The frequencies are calculated from (20). These methods are termed MARES, MGARES, and MGARIVES where the letter E denotes that the exact solution form of curve-fit is used and the letter S denotes that the frequencies are obtained from the purely sinusoidal assumption used to derive (20).

(b) The frequencies are calculated using Prony's method, (10) and (11). These methods are terms MAREP, MGAREP, and MGARIVEP. The letter P denotes that the frequencies are estimated from Prony's method.

In total, 10 different techniques are created in this manner. The remainder of this paper is devoted to the comparison of the performance of these methods. The aim is to understand which approach performs best under what conditions and to eliminate the least promising methods.

7. METHOD EVALUATION USING SIMULATED DATA

In this section the new methods are evaluated using a BTT data simulator. The simulator is a mathematical model of a bladed assembly with any number of blades. The blades are modelled as cantilever beams with two bending modes of vibration; torsion is not considered. The blades are coupled through coupling springs and dampers, representing coupling due to the disc. The simulator is represented graphically in Figure 2 for the special case of four blades. Further details on the mathematics of the simulator are given by the authors [6].

Several exhaustive tests were performed using BTT data obtained from the simulator to evaluate the accuracy of the new methods and their sensitivity to various test parameters. These parameters were the following.

(a) Type of simultaneous resonances, that is, whether the resonances are synchronous or asynchronous. Two cases were considered; one with two simultaneous synchronous resonances and one with one synchronous and one asynchronous resonance.

(b) Percentage of the waveform sampled (probe spacing on the resonance): one of the most important considerations in BTT data analysis is the percentage of one cycle that is measured by the probes. If the percentage is too small, then significant errors can occur in the estimation of the response frequency. If the percentage is too large, then the response may be undersampled, again leading to large errors. The probe spacing on the resonance (PSR) is defined as

$$\text{PSR} = \frac{\text{EO}\gamma}{2\pi}, \tag{35}$$

where EO is the response engine order and γ is the angular distance in radians between the first and last probes. Figure 3 shows a single cycle of a 1-EO resonance sampled by 9 BTT probes at low PSR (16.9%) and at high PSR (80.1%). It is clear that the low PSR data are not very representative of the sine wave response; in fact they could be mistaken to represent a straight line. On the other hand, the high PSR BTT data are clearly samples taken from a sine wave.

(c) Noise levels: the nominal amount of noise in BTT data is around 10% of the root mean square (RMS) value of the blade tip response. However, higher noise levels can be encountered.

Two different assemblies were used in the tests, denoted by Test 1 and Test 2. The first assembly featured two synchronous simultaneous resonances and the second has one

synchronous resonance and one asynchronous resonance occurring nearly simultaneously. The assembly characteristics are summarised in Table 1.

The resulting data simulate acceleration manoeuvres through a range of rotational speeds with constant excitation patterns, that is, engine orders. Notice that from a physical and mathematical point of view, an engine order of 6.5 is meaningless. However, it is a convenient way to approximating asynchronous data using the BTT simulator. Accordingly, the engine order estimates produced by the autoregressive methods for the 6.5 case do not represent a real Engine Order but the ratio of the blade tip response frequency to the assembly's rotational speed. The objective of case T2 is to investigate the performance of the autoregressive methods when an asynchronous vibration phenomenon such as flutter coincides with an engine-ordered resonance.

The resulting BTT data was analysed as the resonance was traversed. The simulated assembly was perfectly tuned as all blades and coupling ratios between the blades were identical. The parameters that define the blade characteristics were kept constant for both test cases.

The natural frequencies of the assembly modes are given in Table 2. Note that, since the assembly is perfectly tuned, the natural frequencies of assembly modes 2 and 3 are identical, that is, these modes are double modes.

The noise sequences were generated from sets of random numbers chosen from a distribution with 0 mean and variance 1. Given an infinite number of entries, the noise sequence would have a mean exactly equal to zero. However, finite sets of data always feature some bias. To ensure that the results obtained from the analysis of each level of noise were not biased, one hundred different sequences of noise sets were generated and added to the BTT data. The 100 sets of corrupted BTT data sequences were then analysed with all the methods and the resulting engine order estimates were processed statistically to yield the average error in engine order estimation, that is,

$$\overline{E} = \frac{1}{100}\sum_{j=1}^{100}\left(\mathrm{EO}_{\mathrm{true}} - \mathrm{EO}_{e_i}\right), \tag{36}$$

where $\mathrm{EO}_{\mathrm{true}}$ is the true engine order and EO_{e_i} is the ith estimated engine order. The standard deviation, σ, of the errors in engine order was calculated as

$$\sigma = \sqrt{\frac{1}{99}\sum_{j=1}^{100}\left(\mathrm{EO}_{\mathrm{true}} - \mathrm{EO}_{e_i} - \overline{E}\right)^2}. \tag{37}$$

7.1. Discussion of results from evaluation A

Evaluation A consisted of varying the PSR values and noise levels simultaneously with the aim to determine the effect of PSR variation upon the ability of the methods to recover the correct frequencies of vibration. Additionally, this evaluation was designed to determine the optimum PSR values to use with the new methods. The evaluation was carried out using test case T1 only, as it is the critical case for which the new analysis methods were developed.

Table 1: Test cases using simulated data.

Trial case	Engine order	Blades
T1	6, 36	4
T2	6.5, 39	4

Table 2: Natural frequencies of assembly modes in Hz.

		Frequency (Hz)	
		Blade mode 1	Blade mode 2
Assembly modes	1	17.0111	105.9959
	2	18.8102	114.9826
	3	18.8102	114.9826
	4	20.0244	123.3862

At each PSR level, the average error in recovered engine order, $\overline{E}$, was calculated over all the noise levels for each method individually. Tables 3 and 4 show $\overline{E}$, as recovered by the MAR method for blade modes 1 and 2, respectively, along with the average $\overline{E}$ (i.e., $\overline{\overline{E}}$) values displayed in the last row of the table. The same procedure was used to calculate the average standard deviation of the recovered engine orders, $\overline{\sigma}$. The $\overline{E}$ results obtained that are below 2%, that is, 0.02 are considered as acceptable errors. A 2% bias error means that solutions up to 25 EOs would yield a correct result. The results above 2% error have been shaded in the tables. Figure 4 shows that, for mode 1, acceptable solutions are obtained for progressively higher noise levels as the PSR is increased. For the second mode (Figure 5), if the PSR is increased beyond 55%, the errors start increasing again. All the recovered solutions from all the methods were processed in the same way.

Table 5 shows a summary of the PSR values for which the minimum average $\overline{E}$ was obtained. Similarly, the PSRs yielding the lowest average values of the standard deviation were extracted. It can be seen from the table that for the resonance corresponding to blade mode 1, all the methods recover the least average error ($\overline{E}$) at 80% PSR. However, for blade mode 2 the Prony-based methods yield better results between 45% and 60% PSR; the techniques using the exact solution (EP/ES) obtain the best results at 50% PSR exactly. The lowest average $\overline{\sigma}$ occurs at the highest tested PSR value for both blade modes.

Table 6 summarises for each method the PSR values for which the $\overline{\overline{E}}$ and $\overline{\sigma}$ results remained below 10% for both modes. The PSR value at which $\overline{\overline{E}}$ is below 10% differs from method to method, but for most techniques this limit is at a PSR setting close to or above 30%. The average $\overline{E}$ results for the second mode deteriorate for PSR settings above 70% for nearly all methods. Average $\overline{\sigma}$ values below 10% were obtained for PSR settings above 20% for nearly all methods.

The main conclusion to be drawn from evaluation A is that all methods can yield good estimates of the response engine orders as long as the PSR value lies between 40 and 70%, with the optimum accuracy for both simultaneous responses occurring at a PSR of 50%.

Table 3: MAR $\overline{E}$ results for mode 1 at for different noise level and PSR%.

MAR	Mode 1 $\overline{E}$														
AC noise level	PSR														
	10	15	20	25	30	35	40	45	50	55	60	65	70	75	80
0	331.24	21.21	0.90	0.67	0.22	0.16	0.10	0.06	0.08	0.09	0.08	0.07	0.07	0.07	0.06
5	539.85	473.30	458.95	224.02	12.47	0.72	0.07	0.06	0.13	0.03	0.03	0.03	0.11	0.05	0.10
10	534.23	491.01	506.80	318.28	49.64	3.03	0.49	0.08	0.13	0.28	0.09	0.02	0.08	0.10	0.05
15	566.69	503.96	532.94	371.36	94.88	8.85	0.32	0.13	0.39	0.28	0.20	0.16	0.06	0.25	0.00
20	542.05	547.97	532.77	429.82	141.61	18.82	0.25	0.02	0.43	0.66	0.05	0.06	0.09	0.34	0.09
25	586.30	560.41	551.27	437.48	162.96	25.97	2.62	0.90	0.68	0.75	0.32	0.56	0.77	0.78	0.08
30	571.92	608.89	547.27	450.82	201.72	44.93	3.44	2.04	2.06	1.47	0.19	0.02	1.15	0.86	0.10
35	579.82	610.38	562.47	446.90	237.68	48.22	8.37	2.27	3.13	2.35	1.00	1.06	0.95	0.55	0.10
Average, $\overline{\overline{E}}$	531.51	477.14	461.67	334.92	112.65	18.84	1.96	0.70	0.88	0.74	0.24	0.25	0.41	0.37	0.07

Table 4: MAR $\overline{E}$ results for mode 2 at for different noise level and PSR%.

MAR	Mode 2 $\overline{E}$														
AC noise level	PSR														
	10	15	20	25	30	35	40	45	50	55	60	65	70	75	80
0	13.34	0.24	0.00	0.01	0.00	0.00	0.00	0.00	0.00	0.01	0.01	0.01	9.84	22.51	33.62
5	349.45	69.94	8.83	0.28	0.43	0.04	0.07	0.04	0.00	0.00	0.13	1.73	9.54	22.48	33.63
10	372.77	109.60	16.81	0.02	0.81	0.07	0.25	0.07	0.02	0.02	0.26	2.53	10.07	22.48	33.61
15	374.99	138.12	22.99	0.81	0.26	0.27	0.50	0.09	0.06	0.09	0.94	3.79	10.41	22.64	33.61
20	376.00	159.95	38.09	3.56	0.06	0.45	0.91	0.23	0.06	0.11	1.64	4.51	11.09	22.89	33.57
25	375.49	175.20	46.29	2.46	0.47	1.38	1.15	0.35	0.06	0.04	2.46	5.98	11.57	23.16	33.59
30	374.78	181.31	51.94	5.16	1.04	1.84	1.62	0.49	0.09	0.00	3.17	6.27	11.60	23.52	33.52
35	373.34	190.48	61.06	8.57	2.77	1.96	2.23	0.60	0.08	0.03	3.70	7.15	12.41	23.76	33.63
Average, $\overline{\overline{E}}$	326.27	128.10	30.75	2.61	0.73	0.75	0.84	0.23	0.05	0.04	1.54	4.00	10.81	22.93	33.60

7.2. Discussion of the results from evaluation B

Evaluation B consisted of increasing the noise level from 0 to 35% at a single PSR value, 35%. This value was chosen as it is near the lower end of the validity region for most methods (see Table 6). The results for this evaluation are presented in the form of figures showing the 95% confidence bands recovered by each method for increasing levels of noise. Evaluation B was repeated for the two test cases Test 1 (two simultaneous synchronous resonances) and Test 2 (one synchronous and one asynchronous resonance occurring simultaneously).

Test 1

Results from this test are shown in Figures 4–7. There are two figures for blade mode 1, one showing results from the Prony-based methods and one from the exact methods. Similarly, there are two figures for blade mode 2. The grey bands on the figures show the area within which the results are acceptable. Inaccuracies start to occur when at least one of the confidence bands for a particular method exits this grey area.

It is clear that the exact methods (Figures 5 and 7) perform better than the Prony-based methods (Figures 4 and 6). MGARIV is the best Prony-based method; its confidence bounds remain inside the acceptable area at noise levels up to 20% for blade mode 1 and 35% for blade mode 2. MGARIVES and MGARIVEP are the best exact methods, their predictions remaining acceptable up to the maximum tested noise level of 35%.

Test 2

Results from this test are shown in Figures 8–11. As for Test 1, there are two figures for blade mode 1, (Prony-based and exact methods) and two figures for blade mode 2. In this case it is harder to separate the performance of the Prony-based methods from that of the exact approaches. On balance, the Prony-based techniques appear to yield more accurate results for the asynchronous engine order while the exact methods are more accurate for the synchronous engine order.

The best Prony-based approach for Test 2 is again MGARIV, yielding predictions within the acceptable region at noise levels of up to 30% for mode 1 and 35% for mode 2. MGARIVEP is the best exact method for Test 2, remaining accurate up to noise levels of 35% for both mode 1 and mode 2. Note that for Test 1 the results from MGARIVEP and MGARIVES are virtually identical. This is not the case for the asynchronous mode of Test 2.

Test 2 was repeated for a PSR of 50%, which is the PSR for which most of the methods yield their best predictions

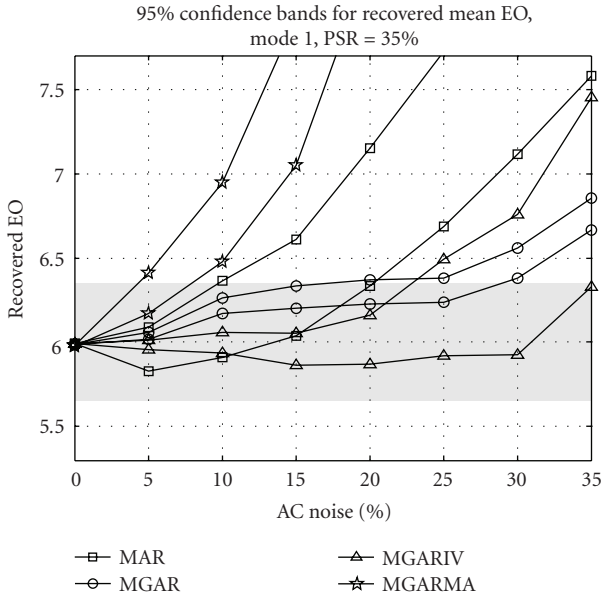

Figure 4: Test 1: 95% confidence bands for Prony-based methods, mode 1.

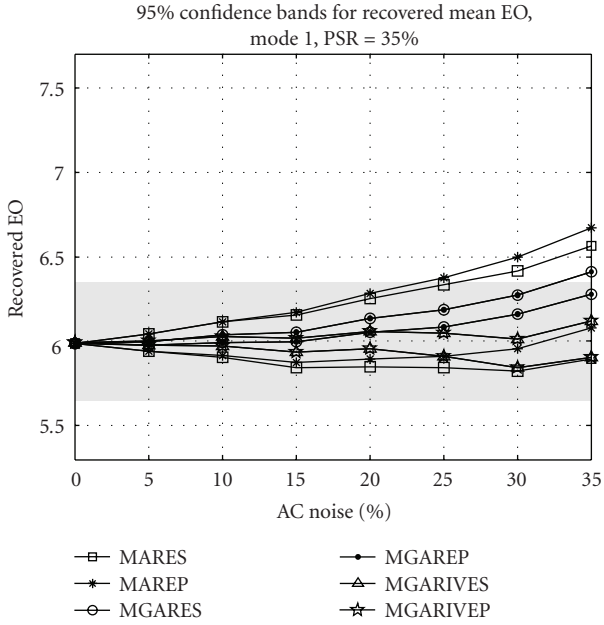

Figure 5: Test 1: 95% confidence bands for exact solution methods, mode 1.

for blade mode 2 and very good predictions for blade mode 1 (see Tables 5 and 6). For this PSR, all the methods had confidence bands within the acceptable regions for both modes up to a noise level of 35%.

8. CONCLUSIONS

A class of autoregressive-based methods for the analysis of blade tip timing data from assemblies undergoing two simultaneous resonances has been developed. The basis of all the approaches is the assumption that the blade tip response can be represented as the response of a dynamic system with two modes. For the simplest method, an autoregressive model is used to represent the blade tip response over a single revolution of the assembly. More complex methods use data from multiple revolutions, an instrumental variable technique and an autoregressive moving average methodology.

The autoregressive coefficients are calculated using least squares curve-fits. Two curve-fitting schemes have been developed; one where all the autoregressive coefficients are considered unknown and the response frequencies are calculated using Prony's method and one where only two autoregressive coefficients are unknown and the response frequencies are estimated using the assumption that the blade tip response is sinusoidal.

The performance of the methods was evaluated and compared using data from a mathematical BTT data simulator. The sensitivity of the approaches to probe spacing on the resonance (PSR) and measurement noise was of particular

Table 5: PSR values for lowest average mean engine order error and average standard deviation of all noise sequences.

Method	PSR yielding the lowest $\overline{\overline{E}}$		PSR yielding the lowest $\overline{\sigma}$	
	Mode 1	Mode 2	Mode 1	Mode 2
MAR	80	55	80	80
MGAR	80	60	80	80
MGARIV	80	45	80	80
MGARMA	80	50	80	80
MARES	80	50	80	80
MAREP	80	50	80	80
MGARES	80	50	80	80
MGAREP	80	50	75	80
MGARIVES	80	50	75	80
MGARIVEP	80	50	75	80

Table 6: PSR values at which acceptable results were obtained for both modes.

Method	PSR (%) yielding $\overline{\overline{E}} < 10\%$	PSR (%) yielding $\overline{\overline{\sigma}} < 10\%$
MAR	40 to 70	>10
MGAR	35 to 70	>22
MGARIV	35 to 70	>19
MGARMA	50 to 68	>21
MARES	30 to 70	>19
MAREP	35 to 70	>19
MGARES	30 to 70	Any
MGAREP	30 to 70	Any
MGARIVES	20 to 70	>19
MGARIVEP	25 to 70	>19

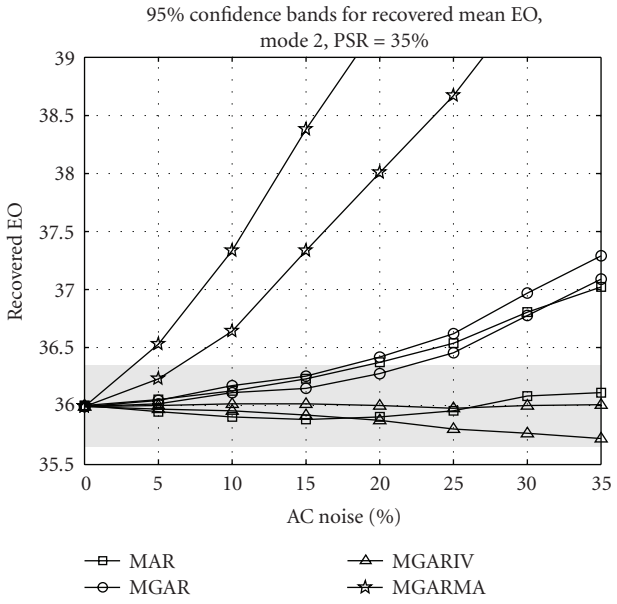

Figure 6: Test 1: 95% confidence bands for Prony-based methods: mode 2.

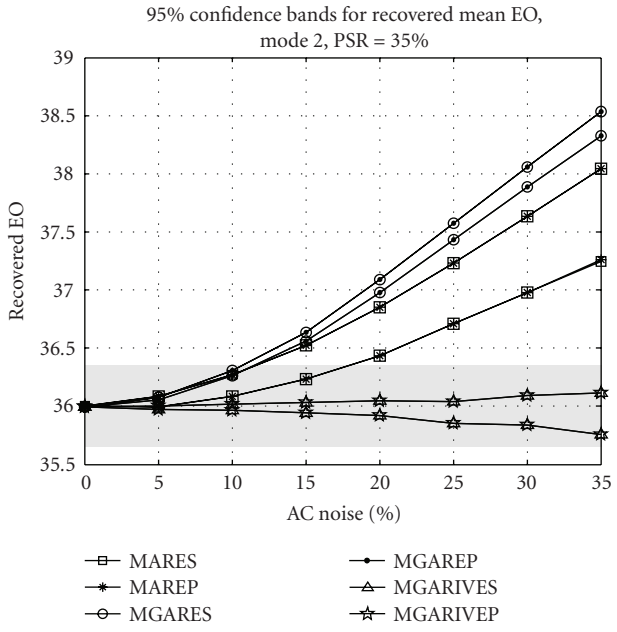

Figure 7: Test 1: 95% confidence bands for exact solution methods, mode 2.

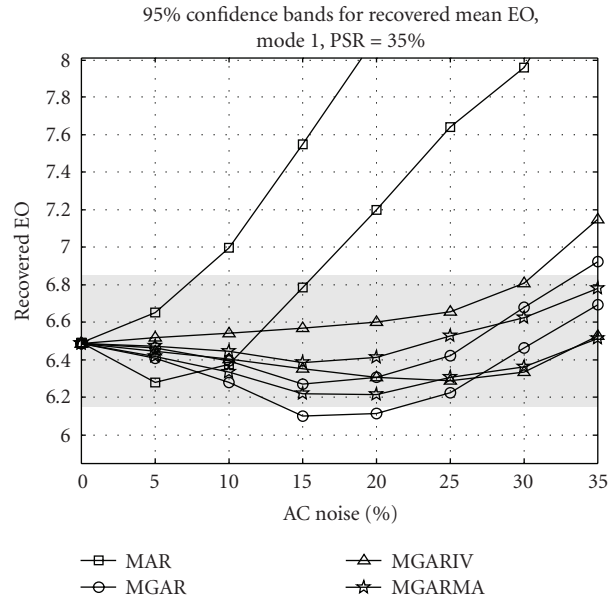

Figure 8: Test 2: 95% confidence bands for Prony-based methods, mode 1.

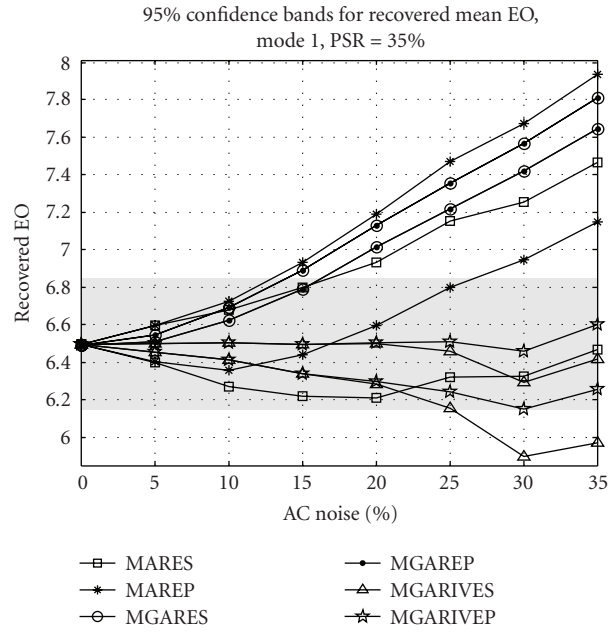

Figure 9: Test 2: 95% confidence bands for exact solution methods, mode 1.

interest. It was shown that increasing PSR has different effects for the low frequency and high frequency modes. For the lower frequency mode, bias and scatter are reduced as the PSR is increased. For the higher mode, bias is reduced until a PSR value where the optimum accuracy is obtained. At PSRs higher than this value bias increases, although scatter continues to decrease. A PSR of 50% yields accurate engine order predictions for both modes under investigation and is considered to be an optimum choice. MGARIVES and MGARIVEP exhibited the broadest PSR ranges within which highly accurate frequency estimates can be obtained.

The instrumental variables formulations (MGARIV, MGARIVES/EP) are significantly better than the other methods, both in terms of bias and scatter. MGARIV is most accurate when analysing asynchronous resonances while MGARIVEP is most accurate for synchronous resonances. The poor results obtained from the MGARMA method are

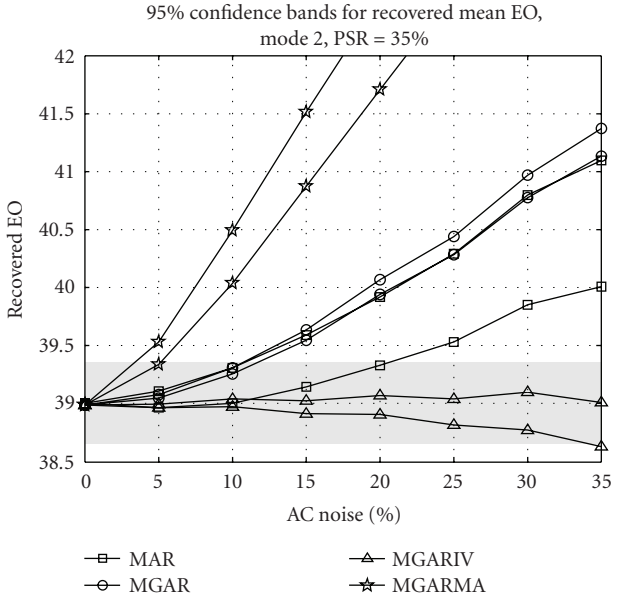

Figure 10: Test 2: 95% confidence bands for Prony-based methods, mode 2.

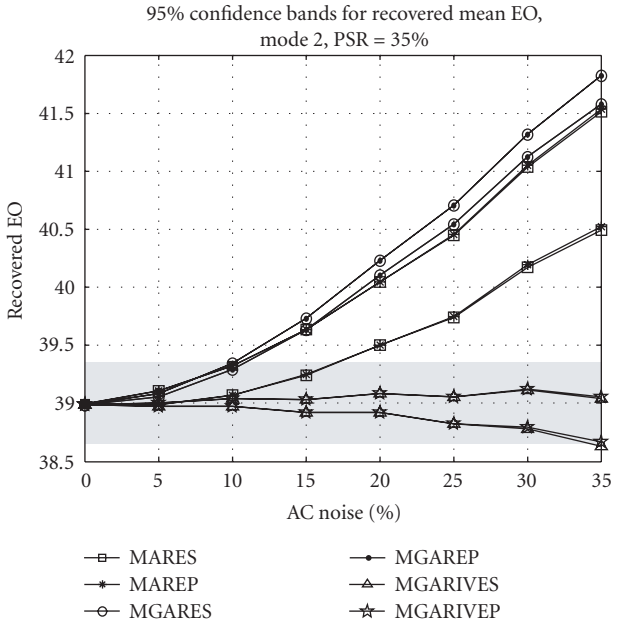

Figure 11: Test 2: 95% confidence bands for exact solution methods, mode 2.

most likely due to the attempt to create a noise model from data with such a low sampling rate.

The MGARIVES/EP and MGARES/EP pairs yield almost identical frequency estimates for all cases. Therefore, only one of each pair should be considered for further applications to real-life problems.

Part II of this paper will show examples of experimental application of the new methods.

ACKNOWLEDGMENTS

The authors would like to thank Rolls-Royce PLC and the Engineering and Physical Sciences Research Council of the UK.

REFERENCES

[1] I. Ye Zablotskiy and Yu. A. Korostelev, "Measurement of Turbine Blades with the ELURA Device," 1970, Energomashinostroneniye, Nr. 2, February 1970, pp. 36–39, English version: U.S. Air Force Systems Command Foreign Technology Division, FTD-ID(RS)T-0861-78, June 1978, AD-A066122.

[2] S. Heath, T. Slater, L. Mansfield, and P. Loftus, "Turbomachinery blade tip-timing measurement techniques," in *Proceedings of Advisory Group for Aerospace Research and Development Conference, 90th Symposium on Advanced Non-Intrusive Instrumentation for Propulsion Engines*, pp. 32-1–32-9, Brussels, Belgium, October 1997.

[3] M. Zielinski and G. Ziller, "Noncontact vibration measurements on compressor rotor blades," *Measurement Science and Technology*, vol. 11, no. 7, pp. 847–856, 2000.

[4] G. Dimitriadis, I. B. Carrington, J. R. Wright, and J. E. Cooper, "Blade-tip timing measurement of synchronous vibrations of rotating bladed assemblies," *Mechanical Systems and Signal Processing*, vol. 16, no. 4, pp. 599–622, 2002.

[5] I. B. Carrington, J. R. Wright, J. E. Cooper, and G. Dimitriadis, "A comparison of blade tip-timing data analysis methods," *Proceedings of the Institution of Mechanical Engineers—Part G: Journal of Aerospace Engineering*, vol. 215, no. 5, pp. 301–312, 2001.

[6] J. Gallego-Garrido, G. Dimitriadis, and J. R. Wright, "Development of a multiple modes simulator of rotating bladed assemblies for blade tip-timing data analysis," in *Proceedings of the 27th International Conference on Noise and Vibration Engineering (ISMA '02)*, pp. 1437–1446, Leuven, Belgium, September 2002.

[7] J. Gallego-Garrido and G. Dimitriadis, "Validating synchronous blade vibration amplitudes from blade tip-timing data analysis," in *Proceedings of the 8th International Conference on Vibrations in Rotating Machinery*, vol. 2, pp. 205–214, Swansea, UK, September 2004.

[8] E. K. Armstrong and R. E. Stevenson, "Some practical aspects of compressor blade vibration," *The Journal of the Royal Aeronautical Society*, vol. 64, no. 591, pp. 117–130, 1960.

[9] W. W. Robinson, "Overview of Pratt & Whitney NSMS," in *Proceedings of the 45th International Instrumentation Symposium*, Albuquerque, NM, USA, May 1999.

[10] W. W. Robinson and R. S. Washburn, "A Real Time Non-Interference Stress Measurement System (NSMS) for Determining Aero Engine Blade Stresses," Instruments Society of America, 1991, paper 91-103, pp. 793–811.

[11] H. T. Jones, "Development of advanced non-intrusive stress measurement processing techniques," in *Proceedings of the 6th National Turbine Engine High Cycle Fatigue Conference*, Jacksonville, Fla, USA, May 2001.

[12] B. W. Hayes, S. Arnold, C. Vining, and R. Howard, "Application of generation 4 non-contact stress measurement systems on HFC demonstrator engines," in *Proceedings of the 9th National Turbine Engine High Cycle Fatigue Conference*, Pinehurst, NC, USA, March 2004.

[13] S. L. Marple, *Digital Spectral Analysis: With Applications*, Prentice-Hall, Englewood Cliffs, NJ, USA, 1987.